

A Highly Sensitive Force Sensor with Fast Response Based on Interlocked Arrays of Indium Tin Oxide Nanosprings toward Human Tactile Perception

Sungwoo Chun, Il Yong Choi, Wonkyeong Son, Gi Yoon Bae, Eun Jae Lee, Hyunah Kwon, Jaimyun Jung, Hyoung Seop Kim, Jong Kyu Kim,* and Wanjun Park*

Development of a sensor for recognizing tactile feeling is essential for realizing artificial systems that can perform human tactile functions for various applications. For achieving the capability of human tactile sensation, highly sensitive responses are required not only to static pressures but also to dynamic high-frequency vibrations. Here, a highly sensitive force sensor based on interlocked arrays of vertically aligned indium tin oxide (ITO) nanospring structures fabricated on a flexible polyethylene naphthalate substrate is presented. The combination of rigid ITO on the flexible substrate, its unique nanoscale spring-like geometry, and the interlocking configuration results in sensitive responses to both static and dynamic pressures with a sub-millisecond response time over wide pressure and frequency ranges appropriate for human tactile perception. Consequently, the sensor is capable of classifying eight fabrics possessing complex patterns with 99.8% accuracy. In addition, a flexible 14 × 14 force sensor matrix array is demonstrated, thus demonstrating the integration capability.

1. Introduction

Development of a sensor recognizing tactile feeling, one of the five human senses, is essential for realizing artificial systems with implemented human tactile functions for various applications such as robotics, healthcare monitoring, wearable electronics, human–machine interfaces, and prosthetics.^[1–7] The tactile perception by cutaneous mechanoreceptors in human skin is not a static process influenced only by the force applied on the surface of an object, but a dynamic process in which both force and vibration, as skin slides across a surface, enable the discrimination of the surface texture and the softness of a material.^[8] Therefore, development of a tactile

sensor capable of human tactile perception requires a highly sensitive detection over wide ranges of vibration as well as pressure, which is challenging to achieve.


Much efforts have been reported to realize tactile sensing devices with sensitive static and dynamic pressure detection capability by introducing ferroelectric, triboelectric, and piezoelectric characteristics.^[9–11] However, extension of these approaches to tactile sensor is limited because recognition of pressure requires an additional sensor element or operating mechanism for force detection. A highly sensitive force sensor can be a strong candidate for a tactile sensor only if its response time is sufficiently fast to distinguish the differences in the interacting vibrations. There have been many studies

on force sensors with various combinations of sensing materials—typically polymeric materials for sensitivity and flexibility—and their nano/micro structures.^[2–4,12–20] However, most of the studies mainly focused on improving the pressure sensitivity. Meanwhile, the capability to detect high-frequency vibrations has been limited owing to the inherently slow responses of the sensors based on polymeric materials for deformation and recovery. In addition, the pressure detection range with high sensitivity is very narrow in comparison with the general pressure range of the human tactile perception, which significantly limits the application of such force sensors in tactile sensing devices. Development of an appropriate combination of a sensing material and its relevant nano/microstructural design is necessary to overcome such limitations to realize a tactile sensor mimicking the human tactile feeling.

Here, we present a flexible, highly sensitive force sensor with sub-millisecond (ms) response based on interlocked arrays of vertically aligned indium tin oxide (ITO) nanospring (NS) structures on a flexible polyethylene naphthalate (PEN) substrate. The combination of the rigid and conductive ITO and the unique nanoscale mechanical interlocking of the NS arrays enables high sensitivities and ultrafast responses with excellent reproducibility and cycling stability to both static and dynamic vertical pressures over a wide range of pressure and frequency. In addition, an integrated sensor matrix array equipped with ridged line patterns emulating the human finger print is presented to demonstrate the detection capability of the sensor

Dr. S. Chun, W. Son, G. Y. Bae, Prof. W. Park
Department of Electronics and Computer Engineering
Hanyang University
222 Wangsimni-ro, Seongdong-gu, Seoul 04763, Republic of Korea
E-mail: wanjun@hanyang.ac.kr

I. Y. Choi, E. J. Lee, Dr. H. Kwon, J. Jung, Prof. H. S. Kim, Prof. J. K. Kim
Department of Materials Science and Engineering
Pohang University of Science and Technology (POSTECH)
77 Cheongam-ro, Nam-gu, Pohang 37673, Republic of Korea
E-mail: kimjk@postech.ac.kr

 The ORCID identification number(s) for the author(s) of this article can be found under <https://doi.org/10.1002/adfm.201804132>.

DOI: 10.1002/adfm.201804132

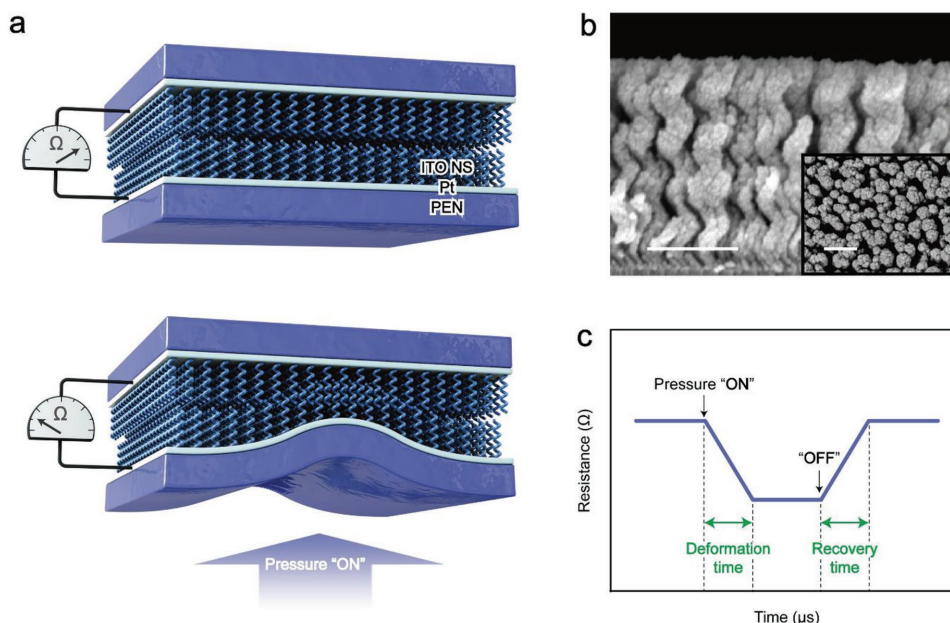


Figure 1. Force sensor based on an interlocking array of ITO NS structures. a) Schematic illustrations of the assembly and operation of the force sensor. The force sensor was fabricated by sandwiching two independently prepared panels containing the array of the vertically aligned ITO NS structures on Pt/polyethylene naphthalate (PEN) substrate. b) Cross-sectional (and top-view in the inset) SEM of the array of ITO NS structures. Each scale bar is 500 nm. c) Schematic illustration of the change in resistance in the force sensor with pressure “ON” and “OFF” operation. The application of external pressure induces the decrease in resistance due to the increase of interlocking displacement.

over working ranges of human tactile perception in terms of pressure, vibration, and scan speed. Finally, we demonstrate an integration capability of the force sensor, and show that the present sensor is capable of recognizing fabrics with eight different complex patterns with 99.8% classification accuracy, which is enabled by its high pressure sensitivity as well as the unprecedented fast response time.

2. Results and Discussion

Figure 1a shows schematic illustrations of the assembly and operation of the force sensor in which two independent arrays of ITO NSs on Pt/PEN substrates are sandwiched. The array consists of uniformly distributed yet isolated individual ITO NSs with $\approx 1.2 \mu\text{m}$ height and $\approx 120 \text{ nm}$ diameter, as shown in the cross-sectional scanning electron microscopy (SEM) (Figure 1b). The arrays on the upper and lower substrates could interlock when an external pressure is applied, in which a tiny displacement between the interlocked high-density NSs in response to the position- and time-dependent external pressure can be sensitively detected as a change in electrical resistance with a response time delay during deformation and recovery, as schematically shown in Figure 1c.

Piezoresistive responses of the force sensors for static vertical pressures were investigated (Figure 2a). Weights were applied on the contacting area of $1 \times 1 \text{ cm}^2$ to generate testing pressures over the range of 100–18 000 Pa which corresponds to the frequently encountered pressure detection range of human tactile perception. The applied pressure induces a change in the interlocking displacement between the upper and lower facing arrays of the ITO NS structures, thus resulting in an increase in the

conductance (G) from the initial conductance (G_0). The sensitivity (S) is defined as $S = (\Delta G/G_0)/\Delta P$, where ΔG is the change in the conductance ($G - G_0$) in response to the change in the applied vertical pressure (ΔP). Note that the measured sensitivity does not increase linearly with increasing pressure, which is consistent with a previously published result.^[2] In the pressure range lower than 6 kPa, the sensitivity (S_1) is estimated to be 3.1 kPa^{-1} through a linear fit. When the vertical pressure is increased from 6 to 18 kPa, the sensitivity (S_2) is enhanced to 15.4 kPa^{-1} , much greater than that observed at the lower pressure range. The change in the sensitivity with applied pressure can be attributed to different interlocking behaviors of the ITO NS structures. In the low pressure range, the arrays of ITO NS structures between the upper and the lower panels undergo an initial stage of interlocking, whereby an appropriate alignment and electrical contact between the ITO NSs begins to occur under the applied force, leading to decreased resistance. Once the alignment and electrical contact are stabilized at a certain pressure close to 6 kPa, the sensitivity (S_2) increases abruptly owing to the increase in the conductance directly caused by the interlocking displacement between the facing arrays of the ITO NS structures. The vertical pressure (18 kPa) is the maximum pressure for the operation of the sensor, induced by the resistance limit of ITO and Pt metal contact when the ITO-NHs and the lower Pt electrode on the opposite side are in contact under external pressure. Note that the force sensor, despite possessing a rigid ITO sensing layer, shows sensitivities of 3.1 kPa^{-1} (for 0.1–6 kPa) and 15.4 kPa^{-1} (for 6–18 kPa), much greater than those of previously reported force sensors based on polymeric sensing materials.^[12,21–23] Such high sensitivities over a wide range of pressure can be attributed to the unique nanoscale spring-like structures that facilitate enhanced elasticity (See finite element method

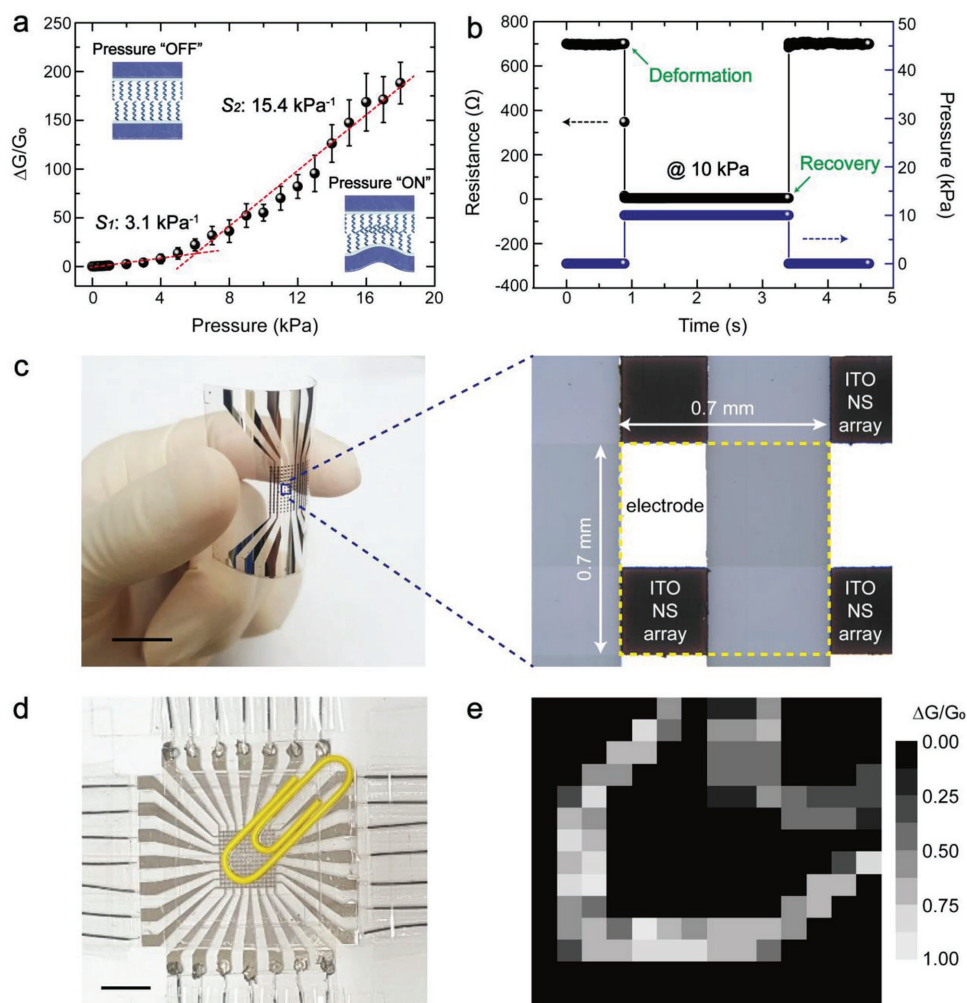


Figure 2. Piezoresistive responses by static and dynamic vertical pressures. a) The sensor response characteristics for pressures induced by the static vertical pressures ranging from 100 to 18 000 Pa. The responses data was acquired from three samples with in the average and the standard deviation. b) The change in the resistance and the applied pressure of the interlocking structure corresponding to a pressing-and-releasing operation. The estimated response time is as fast as 2 ms for deformation and 1 ms for restoration with the applied pressure of 10 kPa. The data points were acquired at the time interval of 1 ms during the pressing-and-releasing operation. c) An array of the indium tin oxide (ITO) NS structures with 196 pixels (14 × 14 sensor matrix) on an area of ≈1 cm². The extended optical image shows a single cell with an area of 0.7 mm × 0.7 mm. d) The completed sensor array with a document clip (1.18 g) placed on the sensor array. e) Spatial image from the sensor responses for the document clip.

simulation results described in Tables S1 and S2 and Figure S1 in the Supporting Information), which aids in overcoming the drawbacks such as the low sensitivity and poor flexibility of rigid materials, yet maintaining their significantly excellent high-frequency property.

Figure 2b shows the change in the resistance of the interlocking structure accompanying a pressing-and-releasing operation. Using the application and the recovery time delay of applied pressure and data points in the interval of 1 ms, we were able to estimate the time for deformation to be less than 2 ms, and that for restoration less than 1 ms, indicating that the sensor can detect vibrating pressures up to 1 kHz with negligible signal loss. This is comparable to the frequency range (<400 Hz) of human perception for tactile sensing through the detection of vibrations.^[24–26] Such a fast response time is attributed to the inherently fast self-recovery enabled by the elastic spring-like structure of rigid ITO. Note that the sub-ms

response time is unprecedentedly fast, and could be hardly achieved from force sensors based on polymeric materials and typical nanostructures. The sensing performance of our sensor is compared with those of previously reported high-performance flexible force sensors summarized in Table S3 (Supporting Information), which reveals that our sensor shows superior performance in terms of the pressure sensitivity in high pressure ranges, as well as the response over wide ranges of vibrations and force, appropriate for human tactile perception. It is attributed to the combination of rigid ITO on the flexible substrate, its unique nanoscale spring-like geometry, and the interlocking configuration.

The force sensor exhibits sensitive and reliable piezoresistive responses to dynamic vertical pressures of 4, 8, 10 kPa for five consecutive pulses (0.7 s) with 1 ms measurement intervals (Figure S2, Supporting Information). In addition, the sensor shows consistent responses to wide range of dynamic

vertical pressures, excellent stability in responses for repetitive operation of 6000 loading–unloading cycles under the vertical pressure of 10 kPa (Figure S3, Supporting Information). This indicates that the array of NSs is robust enough to withstand structural damage that may be caused by the applied forces. This is directly confirmed by comparing the images of the array before and after the application of pressure more than 1000 times (Figure S4, Supporting Information). The force sensor is capable of detecting an extremely small pressure (≈ 4 Pa), which was applied by a weight (0.4 mN) on an area of 1 cm^2 (Figure S5, Supporting Information). For bending strain, this sensor using interlocked arrays of rigid ITO NS structures is flexible enough to be applied as soft electronics (Figure S6, Supporting Information). Moreover, the force sensor with ITO NS structures is robust enough to be insensitive to the external impulses generated by hitting and twisting, after interlocking (Figure S7, Supporting Information). Our sensor shows a high signal-to-noise ratio (SNR) above 20 dB in vibrating pressures for the range of 1–1000 Hz (Figure S8, Supporting Information), indicating that the sensor can resolve the difference of induced vibration beyond the vibration range that a human can detect.

Since the oblique angle deposition (OAD) method is simple, reproducible, and compatible with microelectronic processes, the integration of the force sensors with various microelectronics components on demand can be easily accomplished. In contrast, it is difficult to adopt the integration process for fabricating a sensor array to most force sensors based on polymeric materials. A flexible 14×14 sensor matrix was produced on an area of $\approx 1\text{ cm}^2$, as shown in Figure 2c. The magnified optical image is included to describe the single unit sensor cell with an area of $0.7 \times 0.7\text{ mm}^2$. The spatial resolution of 0.7 mm was chosen to build an equivalent situation of the human fingertip in which mechanoreceptors are mostly distributed with a spatial resolution of 1 mm.^[27] The sensor array was fabricated using conventional optical lithography technology, followed by the construction of the ITO NS structures by OAD. Figure 2d,e shows the spatial recognition of a document clip placed on the sensor array. Its weight and area contacted on the array are $\approx 1.18\text{ g}$ and $\approx 25.45\text{ mm}^2$, respectively corresponding to the vertical pressure of $\approx 460\text{ Pa}$.

Using such promising capabilities offered by our sensor, we now demonstrate the ability of recognizing complex and irregular textures of contacted surfaces. Schematic illustrations showing the operation of force sensor combined with a fingerprint structure (FPS) for recognizing the texture of a surface with rubbing motion, which is analogous to human tactile perception by touching and rubbing the surface of an object, are shown in Figure 3a. The SEM image for periodic FPS pattern was shown in Figure S9 in the Supporting Information. Rubbing of a textured object having a roughness pattern ($L = \text{width} + \text{pitch}$) with a rubbing velocity (v) on a periodic FPS pattern on the force sensor generates time-dependent electrical output signals by an interacting vibration between the FPS and the surface roughness. With fast Fourier transfer (FFT) to obtain the frequency response ($f = v/L$), periodicity information of the roughness patterns, i.e., the surface texture is recognized. The response performance was first evaluated by measuring the interacting vibrations induced by single PET tip (width = $120\text{ }\mu\text{m}$) scanned on the FPS of the sensor with a constant speed. The changes

in the electrical responses due to the touching event at a scanning speed of 1.86 mm s^{-1} (v) in both directions on the sensor are clearly identified by the periodic wave packet over time, as shown in Figure 3b. This periodic response is sufficient to obtain geometrical information about the FPS through the FFT analysis, as shown in Figure 3c. The periodic pattern ($L \approx 600\text{ }\mu\text{m}$) of the FPS is represented at the peak position ($f_0 \approx 3\text{ Hz}$) as $L = v/f_0$. Note that the complete periodic output is attributed to the ability of our sensor to detect the interacting vibrations produced by local and subtle pressure change with a high SNR. Our sensor can detect periodic distances of the ridge patterns down to $100\text{ }\mu\text{m}$ in the FPS and different scan velocities between 1.86 and 68.8 mm s^{-1} , while maintaining the SNR above 10 dB in the power spectrum (Figures S10 and S11, Supporting Information).

In order to analyze and classify the waveform of the interacting vibrations induced by the physical interaction between our sensor and complex, irregular texture patterns, we introduce a deep learning technique. Eight different fabrics were tested to classify the texture patterns. Figure 3d shows the SEM images of the testing fabrics with different surface textures (Figure S12, Supporting Information). The electrical output signals were obtained by rubbing the fabrics on the sensor with a scanning velocity of 24 mm s^{-1} after a gentle contact ($\approx 10\text{ kPa}$), followed by the FFT (Figure S13, Supporting Information). As displayed in Figure 3e, our sensor successfully classified the fabrics with 99.8% classification accuracy using only the texture information obtained by our sensor (Table S4, Supporting Information). This implies that our sensor is sensitive enough to recognize textures including fine and complex patterns, owing to the ability of our sensor to sensitively detect a fine pressure difference with a fast response time.

3. Conclusion

In summary, we demonstrated a flexible and highly sensitive force sensor for performing tactile sensing using interlocked arrays of ITO NS structures on a flexible polyethylene naphthalate substrate. The force sensor, although its sensing layer comprises rigid ITO, shows sensitivities of 3.1 kPa^{-1} (for 0.1–6 kPa) and 15.4 kPa^{-1} (for 6–18 kPa), much greater than those of force sensors based on polymeric sensing materials. In addition, the sensor shows a sensitive response to high-frequency dynamic vertical pressures due to the sub-millisecond response time for restoration. Using the above abilities, we demonstrated to recognize eight fabrics composed of different fine and complex patterns and we succeeded in completely distinguishing the fabrics with 99.8% classification accuracy. Based on the characteristics demonstrated in this work, the proposed simple architecture based on the interlocked arrays of ITO NS structures is a very promising route for realizing a tactile sensing device mimicking the human tactile functions for various future applications.

4. Experimental Section

Fabrication of Force Sensor Based on Interlocked Arrays of ITO NS Structures: A 100 nm thick platinum (Pt) layer was deposited on a PEN substrate using a sputtering system. The array of 4-turn ITO NS

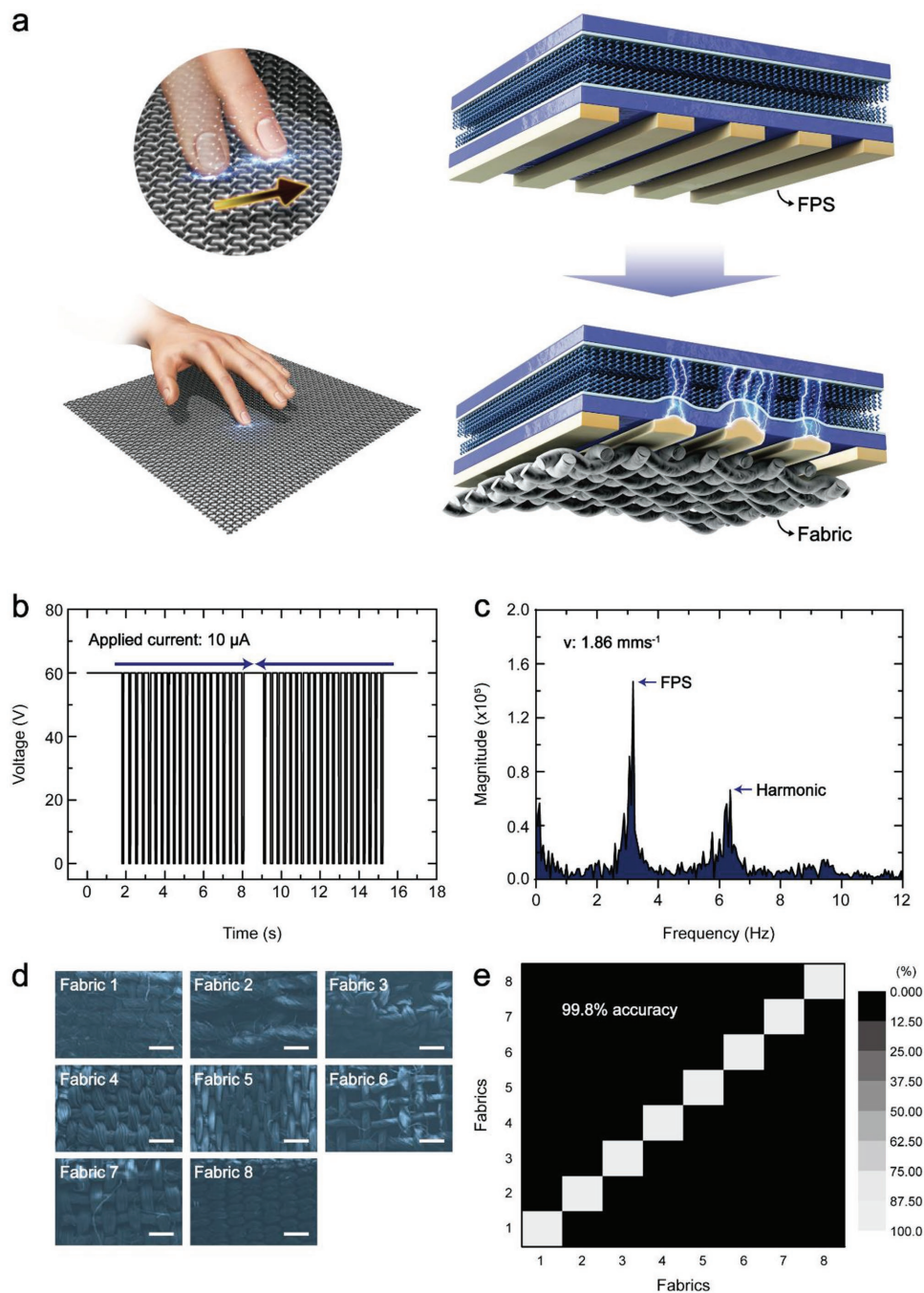


Figure 3. Surface texture recognition with the detection of interlocking vibrations. a) Schematic illustrations showing surface texture recognition by rubbing the sensor combined with a finger print structure (FPS) which is analogous to human tactile perception by rubbing the surface of an object (fabric). The FPS is composed of ridge line patterns (width, 300 μm ; height, 70 μm ; spacing, 300 μm). b) The sensor responses due to the touching event of the single polyethylene terephthalate (PET) tip (width, 120 μm) at a scanning speed of 1.86 mm s^{-1} in both directions. Arrows indicate the forward and reverse direction of slipping, respectively. c) Wave form after fast Fourier transform (FFT) of the sensor responses. d) SEM images of eight fabrics with different surface textures. All the scale bars are 500 μm . e) Confusion matrix for classification in texture with the eight textured fabrics. The individual matrix, visualized by color difference, indicates the probability for classifying one fabric of the eight fabrics with a deep learning method. Total classification accuracy for the eight fabrics is 99.8%.

structures was fabricated on the Pt/PEN substrate using an electron-beam evaporator via the OAD method. This is a simple, reproducible, and microelectronics-compatible approach to form a wide variety of arrays of 3D nanostructures of any evaporable materials on large-area substrates. ITO powder (from Sigma Aldrich) was used for

electron-beam deposition. In the OAD method, the deposition rate and base pressure were maintained at 2.5 \AA s^{-1} and 7.0×10^{-7} Torr, respectively. The tilt angle with respect to the normal axis of the substrate was 85° and the substrate was rotated for 2 s at 1 rpm and stopped for 12 s, repeatedly. The force sensor was fabricated by

sandwiching same two panels of independently prepared ITO NS structures with following procedures: a) Aligning the upper and the lower panel using an optical microscope, b) putting the upper panel on to the lower panel without applying an external force, and c) fixing them by a kapton tape—during this step, the initial resistance was being measured to adjust the fixing force, followed by (d) contact wiring on the each panel. For tactile sensing devices, the FPS was prepared using polyethylene terephthalate (PET). SU-8 photoresist was spin-coated (3000 rpm for 40 s) on the PET surface, followed by a two-step curing process (65 °C for 3 min and 95 °C for 9 min). Optical lithography was performed to form ridge patterns with a height of 70 μm, followed by the conventional reactive ion etching (30 sccm of CH₄ gas and 150 W of plasma power) to obtain a periodic structure with a line width, height, and separation of 300, 70, and 300 μm, respectively. The tactile sensing device was fabricated by attaching the ridge structure on the top surface of the force sensor with appropriate alignment. For obtaining the integrated force sensor array, an array of Pt electrodes was deposited on the PEN substrate using a sputtering system after patterning by conventional photolithography using the AZ 5214 photoresist, followed by a lift-off process with acetone. Then, the PEN substrate with the patterned Pt electrodes was again patterned via conventional photolithography using the AZ 5214 photoresist, followed by OAD using an electron-beam evaporator to form the patterned array (14 × 14) of ITO NS structures. After lift-off process with acetone, two panel of the patterned array with align marks was sandwiched with an accurate alignment using optical microscopy.

Supporting Information

Supporting Information is available from the Wiley Online Library or from the author.

Acknowledgements

S.C. and I.Y.C. contributed equally to this work. This study was supported by the Brain Korea 21 PLUS project of the Center for Creative Industrial Materials (NRF-F17SN25D1706) and the Nano-Material Technology Program (NRF-2016M3A7B4910400) and the Global Ph.D. Fellowship (NRF-2013H1A2A1034492) through the National Research Foundation of Korea (NRF).

Conflict of Interest

The authors declare no conflict of interest.

Keywords

force sensors, nanosprings, tactile classification, tactile sensors, texture recognition

Received: June 15, 2018

Revised: July 31, 2018

Published online: August 30, 2018

- [1] N. Yogeswaran, W. Dang, W. T. Navaraj, D. Shakhivell, S. Khan, E. O. Polat, S. Gupta, H. Heidari, M. Kaboli, L. Lorenzelli, G. Cheng, R. Dahiya, *Adv. Robot.* **2015**, *29*, 1359.
- [2] C. Pang, G. Y. Lee, T. I. Kim, S. M. Kim, H. N. Kim, S. H. Ahn, K. Y. Suh, *Nat. Mater.* **2012**, *11*, 795.
- [3] G. Schwartz, B. C. K. Tee, J. Mei, A. L. Appleton, D. H. Kim, H. Wang, Z. Bao, *Nat. Commun.* **2013**, *4*, 1859.
- [4] T. Q. Trung, S. Ramasundaram, B. U. Hwang, N. E. Lee, *Adv. Mater.* **2016**, *28*, 502.
- [5] S. Jung, J. H. Kim, J. Kim, S. Choi, J. Lee, I. Park, T. Hyeon, D. H. Kim, *Adv. Mater.* **2014**, *26*, 4825.
- [6] A. Chortos, J. Liu, Z. Bao, *Nat. Mater.* **2016**, *15*, 937.
- [7] J. Kim, M. Lee, H. J. Shim, R. Ghaffari, H. R. Cho, D. Son, Y. H. Jung, M. Soh, C. Choi, S. Jung, K. Chu, D. Jeon, S. T. Lee, J. H. Kim, S. H. Choi, T. Hyeon, D. H. Kim, *Nat. Commun.* **2014**, *5*, 5747.
- [8] M. Hollins, S. R. Risner, *Percept. Psychophys.* **2000**, *62*, 695.
- [9] J. Park, M. Kim, Y. Lee, H. Sang Lee, H. Ko, *Sci. Adv.* **2015**, *1*, e1500661.
- [10] L. Lin, Y. Xie, S. Wang, W. Wu, S. Niu, X. Wen, Z. L. Wang, *ACS Nano* **2013**, *9*, 8266.
- [11] W. Wu, X. Wen, Z. L. Wang, *Science* **2013**, *340*, 952.
- [12] S. C. B. Mannsfeld, B. C. K. Tee, R. M. Stoltenberg, C. H. H. Chen, S. Barman, B. V. O. Muir, A. N. Sokolov, C. Reese, Z. Bao, *Nat. Mater.* **2010**, *9*, 859.
- [13] F. R. Fan, L. Lin, G. Zhu, W. Wu, R. Zhang, Z. L. Wang, *Nano Lett.* **2012**, *12*, 3109.
- [14] Q. Shao, Z. Niu, M. Hirtz, L. Jiang, Y. Liu, Z. Wang, X. Chen, *Small* **2014**, *10*, 1466.
- [15] B. C. K. Tee, A. Chortos, R. R. Dunn, G. Schwartz, E. Eason, Z. Bao, *Adv. Funct. Mater.* **2014**, *24*, 5427.
- [16] J. Park, Y. Lee, S. Lim, Y. Lee, Y. Jung, H. Lim, H. Ko, *Bionanoscience* **2014**, *4*, 349.
- [17] J. Park, Y. Lee, J. Hong, Y. Lee, M. Ha, Y. Jung, H. Lim, S. Y. Kim, H. Ko, *ACS Nano* **2014**, *8*, 12020.
- [18] L. Pan, A. Chortos, G. Yu, Y. Wang, S. Isaacson, R. Allen, Y. Shi, R. Dauskardt, Z. Bao, *Nat. Commun.* **2014**, *5*, 3002.
- [19] S. L. Choong, M. B. Shim, B. S. Lee, S. Jeon, D. S. Ko, T. H. Kang, J. Bae, S. H. Lee, K. E. Byun, J. Im, Y. J. Jeong, C. E. Park, J. J. Park, U.-I. Chung, *Adv. Mater.* **2014**, *26*, 3451.
- [20] M. Ha, S. Lim, J. Park, D. E. Um, Y. Lee, H. Ko, *Adv. Funct. Mater.* **2015**, *25*, 2841.
- [21] H. B. Yao, Y. Ge, C. F. Wang, X. Wang, W. Hu, Z. J. Zheng, Y. Ni, S. H. Yu, *Adv. Mater.* **2013**, *25*, 6692.
- [22] H. Park, Y. R. Jeong, J. Yun, S. Y. Hong, S. Jin, S. J. Lee, G. Zi, J. S. Ha, *ACS Nano* **2015**, *9*, 9974.
- [23] J. S. Lee, K. Shin, O. J. Cheong, J. H. Kim, J. Jang, *Sci. Rep.* **2015**, *5*, 7887.
- [24] Y. Shao, V. Hayward, Y. Visell, *Proc. Natl. Acad. Sci. USA* **2016**, *113*, 4188.
- [25] S. Chun, A. Hong, Y. Choi, C. Ha, W. Park, *Nanoscale* **2016**, *8*, 9185.
- [26] R. S. Johansson, F. J. Randall, *Nat. Rev. Neurosci.* **2009**, *10*, 345.
- [27] R. S. Dahiya, G. Metta, M. Valle, G. Sandini, *IEEE Trans. Robot.* **2009**, *26*, 1.